



Solid-state stability studies of cholecystikinin (CCK-4) peptide under nonisothermal conditions using thermal analysis, chromatography and mass spectrometry

Alexis Oliva^{a,*}, David Sánchez Ashen^a, Mario Salmona^b, José B. Fariña^a, Matías Llabrés^a

^a Departamento Ingeniería Química y Tecnología Farmacéutica, Facultad de Farmacia, Universidad de La Laguna, 38200 La Laguna, Tenerife, Spain

^b Istituto di Ricerche Farmacologiche "Mario Negri", Via Giuseppe La Masa 19, 20156 Milano, Italy

ARTICLE INFO

Article history:

Received 8 October 2009
Received in revised form
16 December 2009
Accepted 22 December 2009
Available online 5 January 2010

Keywords:

Solid-state stability
DSC
Nonisothermal kinetic analysis
Peptide cleavage

ABSTRACT

The solid-state stability of cholecystikinin (CCK-4) peptide under nonisothermal conditions was studied by differential scanning calorimetry (DSC), chromatography and mass spectrometry, identifying and schematizing the degradation products. To model the degradation mechanism of the peptide using the combined Kissinger and direct-differential methods, the observed degradation process was characterized by decomposition temperature (T_m), reacted fraction (α_m), activation energy (E_a), and pre-exponential factor (A). Results obtained by the two calculation methods were similar.

The cleavage reaction on both N- and C-terminal sides of aspartic acid was the principal degradation pathway, although the reaction can occur consecutively and/or in parallel. Therefore to determine the relative importance of the different degradation pathways, a system of differential equations relevant to each degradation reaction was analysed using the R[®] statistical program. The results obtained show that the consecutive reaction was the less plausible, whereas a slightly better fit was obtained for the reaction with both processes than for the in-parallel reaction. In this situation, the F -test was applied to discriminate between the models, indicating that the simpler model is the most probable. In conclusion, the results demonstrate for the first time that, in solid-state, $n - 1$ cleavage occurs in parallel to $n + 1$ cleavage at aspartic acid residues and not consecutively.

© 2010 Elsevier B.V. All rights reserved.

1. Introduction

Peptides and proteins may exhibit both chemical and physical degradation also in the state solid (Lai and Topp, 1999), presenting challenges to the pharmaceutical industry during the process of protein purification, formulation, storage and delivery. Understanding peptides and protein degradation pathways is essential for the success of a biopharmaceutical drug. Chemical instability of peptides and proteins can be investigated by different analytical techniques: chromatography, electrophoresis, spectroscopy, thermal analysis, light-scattering and mass spectrometry (Capelle et al., 2007). It is important that these techniques be complemented with methods to assess the biological activity (outside the focus of this article).

Many transformations may occur when a solid sample is heated, such as melting, sublimation, polymorphic transformation, or degradation. These solid-state reactions are quite common in

pharmaceutical science, making the topic of solid-state kinetics important. Solid-state reactions have many forms; however, those that involve weight or enthalpy change are of great interest as their kinetics can be studied by thermal analytical methods (Vyazovkin, 2004; Khawam and Flanagan, 2006a).

DSC has long been applied widely in the pharmaceutical industry and offers a useful means of predicting the solid-state stability of drugs. The DSC experiment can be used to compute the Arrhenius pre-exponential factor, activation energy and order of the reaction (Ford and Timmins, 1989; Beezer et al., 1999; Abd-Elrahman et al., 2002; Pikal et al., 2008).

Kinetics in the solid-state show certain similarities to those in homogeneous phases like solution or gases. In fact, many of the basic mathematical principles are shared among all three phases. However, solid-state reactions differ substantially from those in the homogeneous state regarding the experimental procedures used for their study and computation methods for analysing data (Vyazovkin and Wight, 1999; Giron, 2002; Khawam and Flanagan, 2006b; Sánchez-Jiménez et al., 2008).

The many methods used to study solid-state kinetics may be grouped into two categories: experimental and computational

* Corresponding author.

E-mail address: amoliva@ull.es (A. Oliva).

(Khawam and Flanagan, 2006b). In the first case, there are two approaches used to obtain solid-state kinetic data: isothermal and nonisothermal methods. To analyse data from both of these, model-fitting and model-free methods can be used. Khawam and Flanagan (2006a) have proposed a complementary approach that uses both the latter methods for kinetic data analysis, which allows one to select models that might otherwise be indistinguishable, based on quality of regression fit alone.

The most popular representative of the so-called “model-free” methods is that of Kissinger, which allows the effective activation energy to be determined from the dependence of the peak temperature (T_m) on the heating rate (β). This method provides a single value of the activation energy related to the conversion fraction (α_m) at the peak temperature, and does not require any modelistic assumptions to calculate E_a . However, it is not an isoconversional method because it does not generate E_a at progressive α values but rather assumes a constant E_a .

The Kissinger method can be only applied to the kinetic analysis of rising temperature experiments obtained under any heating schedule when two requirements are fulfilled: a first-order kinetic model is involved and the reacted fraction (α_m) at the maxima remains unchanged (Sánchez-Jiménez et al., 2008).

The choice of isothermal or nonisothermal experiments depends on the requirements of the study, whether one wishes to study reaction kinetics over wide temperature ranges (i.e. up to melting) or if a narrow range is enough. The application of such results to predicting solid-state stability of a drug also affects the choice of the most appropriate reaction conditions.

Calculation methods have also raised many controversies, because there are so many and their range of application and validity is unclear. Results obtained from several of them are often different, even when applied to the same data set. A critical evaluation of these methods was initiated in the ICTAC “kinetic project” (Burnham, 2000; Roduit, 2000).

While the solution reaction of small peptides has been reasonably well characterized (Mu-Lan and Stavchansky, 1998; Joshi and Kirsch, 2002; Oliva et al., 2006a,b), their reactions in the solid-state have attracted scant attention. With the increasing use of small peptides as pharmaceuticals, it is important to understand the solid-state behavior of this type of compounds. The tetrapeptide CCK-4, which constitutes the 30–33 segment of the hormone cholecystokinin, is used in nuclear medicine for the diagnosis of CCK-B receptor-expressing tumors (Gotthard et al., 2004). CCK-4 is a suitable candidate for solid-state studies because of its relatively low cost, but in particular, given its size and structure it can help gain better knowledge of the degradation mechanism of small peptides in the solid-state.

In this study, DSC was used to study the solid-state stability of CCK-4 peptide under nonisothermal conditions. For this, the CCK-4 degradation processes in solid-state, including separation, identification of degradation products, determination of rate constants and degradation pathway were characterized. Kissinger and direct-differential methods were used to analyse the data and estimate the kinetic parameters.

Various models were evaluated and compared to determine the relative importance of the different degradation pathways. Since these models contain more than one kinetic constant that depends on temperature, the number of parameter correlations is larger. To diminish this, the reparameterization of the Arrhenius equation and the proper choice of a reference temperature are of benefit. To estimate the latter, a new norm based on the asymptotic properties of the correlation matrix of a multinormal random variable was proposed.

Table 1

Algebraic expression for the $f(\alpha)$ functions for the most common mechanisms in solid-state reactions.

Model	Symbol	$f(\alpha)$
Zero-order	F0	1
First-order	F1	$(1 - \alpha)$
Second-order	F2	$(1 - \alpha)^2$
Third-order	F3	$(1 - \alpha)^3$
Power law	P2	$2\alpha^{(1/2)}$
Avrami-Erofeev	A2	$2(1 - \alpha)[- \ln(1 - \alpha)]^{1/2}$
Prout-Tompkins	B1	$\alpha(1 - \alpha)$
1-D diffusion	D1	$1/2\alpha$
2-D diffusion	D2	$[- \ln(1 - \alpha)]^{-1}$

2. Theory

Kinetic analysis of solid-state decomposition is usually based on a single-step kinetic equation:

$$\frac{d\alpha}{dt} = k(T)f(\alpha) \quad (1)$$

where t is time, T is absolute temperature, α is the extent of conversion, and $f(\alpha)$ is the reaction model. Table 1 includes the function for the most commonly used mechanisms in solid-state reactions. The explicit temperature dependence of the rate constant is introduced by replacing $k(T)$ with the Arrhenius equation, which gives:

$$\frac{d\alpha}{dt} = Ae^{-E_a/RT}f(\alpha) \quad (2)$$

where A (the pre-exponential factor) and E_a (the activation energy) are the Arrhenius parameters and R is the gas constant.

Under nonisothermal conditions in which a sample is heated at a constant rate, the explicit temporal dependence in Eq. (2) is eliminated through the trivial transformation:

$$\frac{d\alpha}{dT} = \frac{A}{\beta} e^{-E_a/RT} f(\alpha) \quad (3)$$

where $\beta = dT/dt$ is the heating rate, and Eq. (3) represents the differential form of the nonisothermal rate law. The direct-differential method uses Eq. (3) to numerically calculate the differential ($d\alpha/dT \approx \Delta\alpha/\Delta T$). Rearranging the variables and using logarithms in Eq. (3) gives:

$$\ln \left(\frac{d\alpha/dT}{f(\alpha)} \right) = \ln \frac{A}{\beta} - \frac{E_a}{RT} \quad (4)$$

By plotting the left side of Eq. (4) (including the model $f(\alpha)$) against $1/T$, the E_a can be obtained from the slope and A from the intercept. The model that gives the best linear fit is usually chosen as the model (Khawam and Flanagan, 2006a). The universality of Eq. (4) is supported by Ozawa (2000) who previously found it can be applied to data obtained via all modes of temperature change.

Kissinger proposed a kinetic analysis method for reaction-order models ($f(\alpha) = (1 - \alpha)^n$) based on the derivative of Eq. (3), generating $d^2\alpha/dT^2$. Accordingly, the maximum reaction rate occurs when the second derivative is zero, from which the following equation can be obtained:

$$\frac{E_a\beta}{RT_m^2} = A \cdot (n(1 - \alpha_m)^{n-1}) \cdot e^{-E_a/RT_m} \quad (5)$$

where T_m is the temperature and α_m is the conversion fraction at the maximum reaction rate, which represents the peak (i.e. inflection point) of a DSC curve. Taking the natural logarithm of Eq. (5) and rearranging gives:

$$\ln \frac{\beta}{T_m^2} = \ln \left(\frac{AR(n(1 - \alpha_m)^{n-1})}{E_a} \right) - \frac{E_a}{RT_m} \quad (6)$$

The activation energy (E_a) is obtained by plotting the left-hand side of the equation versus $1/T_m$ for a series of runs at different heating rates. Eq. (6) has been generalized to any reaction model ($f(\alpha)$) (Elder, 1985).

3. Materials and methods

3.1. Materials

Cholecystokinin fragment 30–33 amide (CCK-4, Trp-Met-Asp-Phe-NH₂, WMDF-NH₂) was purchased from Sigma Chemical Company (St. Louis, MO, USA). Trp-Met (WM) and Trp-Met-Asp (WMD) peptides were synthesized using Fmoc solid-phase chemistry with a 433A instrument (Applied Biosystems, Foster city, CA) at the Istituto di Ricerche Farmacologiche “Mario Negri”, Milan, Italy, under GMP conditions. Purity was checked by RP-HPLC and MALDI-TOF mass spectrometry. Endoproteinase Glu-C and Modified Endoproteinase Asp-N were purchased from Sigma Chemical Company (St. Louis, MO, USA). Trifluoroacetic acid (TFA: peptide synthesis grade) and acetonitrile (HPLC grade) were obtained from Merck (Darmstadt, Germany). Deionized water was purified in a MilliQ plus system from Millipore (Molsheim, France), prior to use.

3.2. Differential scanning calorimetry (DSC)

DSC experiments were performed in a Mettler Toledo calorimeter, model DSC821^e, with liquid nitrogen cooler and equipped with the Star[®] evaluation program. Calibration of both temperature and enthalpy was made with a standard sample of indium. CCK-4 samples (3–4 mg) were placed in non-hermetically crimped aluminium pans (standard 40 μ L type). The heating rates (β) used for kinetic analysis were 20, 15, 10, 7.5, 5, 2.5 and 1 $^{\circ}$ C/min under nitrogen purge at 30 mL/min. Measurements were carried out on five separate samples (replicates) and reported as averages.

The temperature at maximum rate (T_m) and the conversion fraction (α_m) for each analysis were calculated using the Star[®] software. The α_m value at any temperature is calculated from:

$$\alpha_m = \frac{AUC_0^{T_m}}{AUC_0^{\infty}} \quad (7)$$

where $AUC_0^{T_m}$ is the sample peak area from 0 to T_m , and AUC_0^{∞} is the total sample peak area.

3.3. RP-HPLC method

The chromatographic system used was a Waters apparatus (Milford, MA, USA) consisting of a pump (600E Multisolvant Delivery System), an auto sampler (700 Wisp Model) and a UV-vis detector (2487 programmable multi-wavelength model). Elution was performed at room temperature in a Nova pack C-18 column (150 mm \times 3.9 mm, 60 \AA , 4 μ m particle size, Waters). The data collection and analysis were performed using the Millennium32[®] chromatography program (Waters).

The mobile phase was an acetonitrile–water (30:70, v/v) mixture with 0.05% TFA, the flow rate 1.0 mL/min, and the injection volume 25 μ L. The detection wavelength was set at 280 nm. All solvents were filtered with 0.45 μ m (pore size) filters (Millipore) and degassed.

The analytical method for the three compounds, WMDF-NH₂, WMD, and WM, was validated by selectivity, linearity, limit of detection (LOD), limit of quantitation (LOQ), accuracy, precision and robustness according to the *International Conference on Harmonization (ICH) guidelines (2005)*. The results obtained indicate that the method is specific, linear over a range of concentrations of 2–12 μ g/mL for the three compounds, accurate

(recovery mean < 101.2%), precise (repeatability < 1%), and reliable (inter-assay precision < 4.0%). The LOD was calculated by statistical methods using a ratio of $3\sigma/s$ (σ : the standard deviation of response; s : slope of the calibration curve). The LOQ was also calculated with a ratio of $10\sigma/s$. In all cases, the limits were lower than the smallest concentration in the linearity range. Acceptable robustness was also observed, indicating that the analytical method remains unaffected by small but deliberate variations in mobile phase composition and flow rate, as described in the *ICH Q2-R1 guidelines (2005)*.

3.4. MALDI-TOF mass spectrometry

Mass spectra were measured on an Autoflex MALDI-TOF Mass Spectrometer (Bruker Daltonics, Bremen, Germany), equipped with a 337 nm nitrogen laser, delayed extraction, a reflectron and a hydrophobic coating sample target (Anchor Chip 600/384, Bruker Daltonics, Bremen, Germany). The spectra were obtained using positive ion mode and the accelerating voltage was set to 20 kV. The external calibration of the mass spectrometer was performed with a commercial standard proteins mixture (Bruker Daltonics) and the standard mass deviation was less than 10 ppm. The mass spectra were accumulated for approximately 500 shots per preparation in total, 30 shots each. All reported masses are monoisotopic $[M+H]^+$ unless otherwise noted.

The matrix used was 2,5-dihydroxybenzoic acid (DHB; Sigma) in a saturated solution (0.16 mg/mL in acetonitrile and 0.1% TFA). Samples were deposited on MALDI targets by spotting 0.5 μ L of matrix solution, dried and followed by 0.5 μ L of sample.

3.5. Proteolytic digestion

3.5.1. Sample treatment

CCK-4 peptide (0.1 mg) was dissolved in 100 μ L of DMSO, and afterwards 900 μ L of sodium phosphate (pH=7.8) was added to obtain a final concentration of 100 μ g/mL.

3.5.2. Endoproteinase Glu-C digestion

One 25 μ g vial of endoproteinase Glu-C sequencing grade was reconstituted in 100 μ L double-distilled water. The CCK-4 sample was digested with endoproteinase Glu-C at an enzyme–substrate ratio of 1:100 (w/w) at 25 $^{\circ}$ C for 2 h. Then, 20 μ L of the digested sample was mixed with 180 μ L of mobile phase and analysed by RP-HPLC, the injection volume being 50 μ L.

3.5.3. Endoproteinase Asp-N

Modified Asp-N (*Pseudomonas fragi*, mutant) was supplied lyophilized in a 2 μ g vial, which was reconstituted with 20 μ L double-distilled water, yielding a final enzyme concentration of 0.1 μ g/ μ L. For peptide fragmentation, the enzyme was added to the CCK-4 sample to be digested at a ratio of 1:100 (w/w) at 25 $^{\circ}$ C for 3 h. The peptides obtained by Asp-N digestion were analysed by RP-HPLC using the same conditions as above.

3.6. Identification of degradation products

A sample of CCK-4 was heated up to 210 $^{\circ}$ C, temperature of the maximum rate at 5 K/min, then the sample was quickly cooled to 30 $^{\circ}$ C, and analysed by RP-HPLC. The degradation product peaks were collected by making repeated 200 μ L injections of the degraded sample. Collected fractions were pooled and concentrated in a Speed-Vac[®] before analysis by MALDI-TOF mass spectrometry.

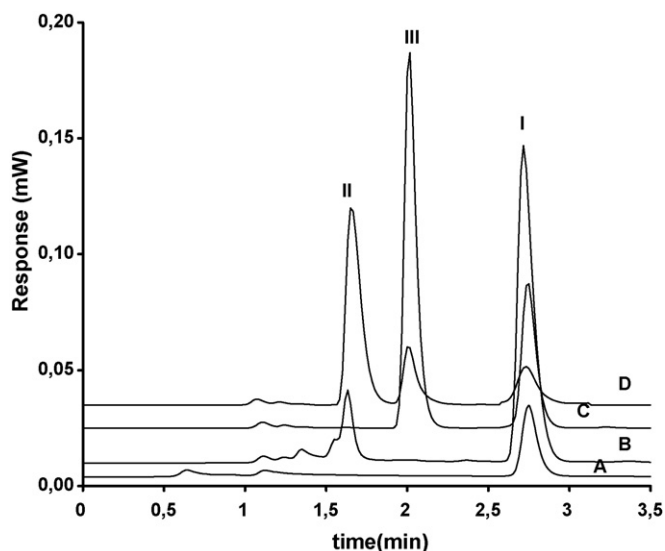


Fig. 1. Chromatograms of CCK-4 sample. (A) Standard sample. (B) Sample hydrolysed using the endoproteinase Glu-C and Asp-N (C), respectively. (D) Sample degraded at 210 °C, two degradation products detected, identified as WMD (II) and WM (III).

3.7. Direct-differential method

Various samples of CCK-4 (2.4–2.6 mg) were analysed by DSC at a heating rate of 5 K/min from 175 to 220 °C at intervals of 5 °C. The rest of the conditions were as described earlier. Each sample was diluted with the mobile phase to obtain concentration values within the calibration range, and analysed by RP-HPLC the same day in duplicate.

In this case, the conversion fraction “ α ” for the WMDF-NH₂ product was calculated from the following expression:

$$\alpha = \frac{m_0 - m_T}{m_0 - m_\infty} \quad (8)$$

where m_0 is the initial sample weight, m_T is the sample weight at temperature T , and m_∞ is the final sample weight. However, the determination of m_∞ is problematic since the residues are totally carbonized above 220 °C. For this reason, m_∞ was taken as zero. For the WMD and WM derivatives, the conversion fraction “ α ” is obtained directly as the sample weight at temperature T .

4. Results and discussion

4.1. Degradation product identities

Degradation products were separated by RP-HPLC and identified by proteolytic digestion and MALDI-TOF mass spectrometry. Chromatographic separation of a degraded CCK-4 sample shows three peaks (I–III, Fig. 1). Peak I was found to have a mass of 596.25, which corresponds to the parent peptide (WMDF-NH₂), while II was found to have a mass of 450.51 (WMD). The difference in mass between peaks I and II was 145.47, which corresponds to the loss of phenylalanine-amide (Phe-NH₂). In addition, the difference in mass between peaks II and III was 115.37, which corresponds to the loss of an aspartic acid residue (WM). This result suggests that the degradation pathway of this peptide in solid-state involves the cleavage reaction on the $n-1$ and $n+1$ sides of aspartic acid. To verify this, CCK-4 samples were hydrolysed using two endoproteinases, Glu-C and Asp-N, and analysed by RP-HPLC. The results confirm that peaks II and III correspond to the WMD and WM fragments, respectively. The degradation

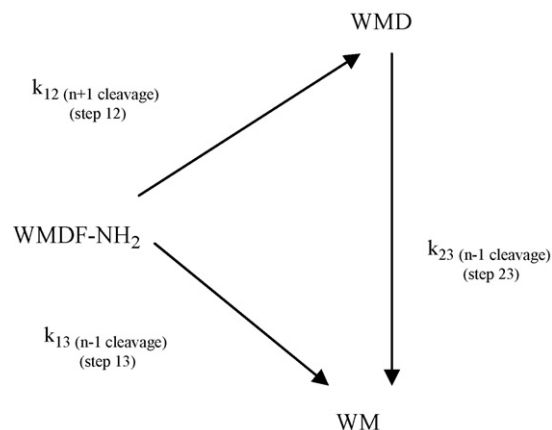


Fig. 2. Degradation scheme proposed for cleavage reaction at aspartic acid residue for the CCK-4 peptide in solid-state. The full model involved the parallel and consecutive pathways of $n+1$ and $n-1$ cleavage reaction.

products and the proposed degradation routes are shown in Fig. 2.

4.2. DSC data

Fig. 3 shows the DSC curve for heating rates of 1, 5 and 10 K/min, which reveals two endothermic peaks in the 190–240 °C. Also clearly visible was the shifting of endothermic peaks to a higher temperature by increasing the heating rate. To identify these two characteristic phenomena, the melting point of CCK-4 was determined using a Buchi instrument (Model B-540, Delaware, USA), obtaining a value of 222.5 ± 0.5 °C ($n=3$) for a heating rate of 5 K/min. Hence, the second DSC endotherm could correspond to the melting point. The first DSC endotherm required more detailed study, so the effects of heating CCK-4 to the different temperatures were compared. A sample of CCK-4 was heated in the DSC up to 175 °C at 5 K/min, before the first DSC endotherm, removed, and then cooled to 30 °C and analysed by RP-HPLC, detecting the

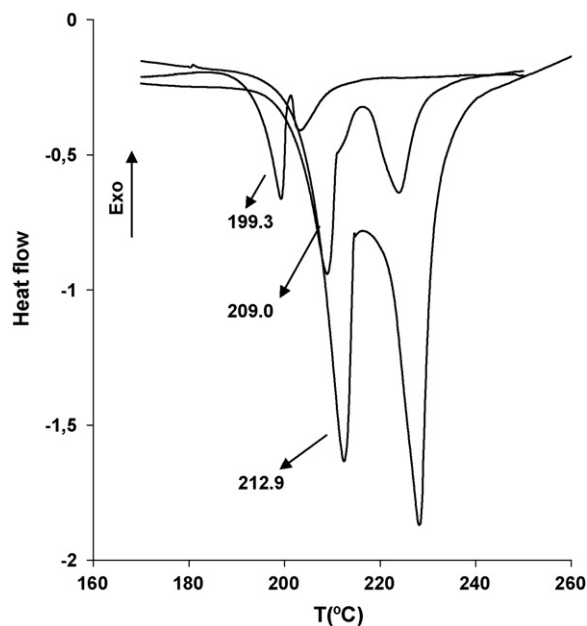


Fig. 3. DSC curves for the CCK-4 peptide at different heating rates ($\beta=1, 5$ and 10 K/min), where the corresponding decomposition temperature, T_m , increases with the heating rate.

Table 2

The peak temperature (T_m) and conversion fraction at peak temperature (α_m) at different heating rates obtained in the decomposition of CCK-4 by DSC.

Heating rate ($^{\circ}\text{C}/\text{min}$)	Peak temperature ($T_m, ^{\circ}\text{C}$)	%Conversion at peak temperature (α_m)
1.0	199.3 \pm 0.26	75.5 \pm 0.26
2.5	204.7 \pm 0.36	75.6 \pm 0.87
5.0	209.0 \pm 0.16	74.4 \pm 0.98
7.5	211.6 \pm 0.18	74.7 \pm 1.11
10	212.9 \pm 0.36	73.8 \pm 0.62
15	216.1 \pm 0.24	74.1 \pm 0.96
20	218.0 \pm 0.42	74.2 \pm 1.13

peak corresponding to pure CCK-4. Another sample of CCK-4 was heated to 210 $^{\circ}\text{C}$, temperature of the maximum rate at 5 K/min, and was similarly analysed. In this case, the degradation products, WMD and WM, were detected. Therefore, the first DSC endotherm is attributed to the solid-state decomposition of CCK-4 according to the diagram shown in Fig. 2. The second endotherm, attributed to the melting of CCK-4, could actually correspond to the melting of both products.

This fact was also observed in other samples of CCK-4 analysed at different heating rates (1, 2.5 and 10 K/min), both degradation products were also detected, indicating that the degradation mechanism can be the same, independently of the heating rate.

The corresponding decomposition temperature, T_m , and the conversion fractions (α_m) obtained for different heating rates are shown in Table 2. Low relative standard deviation values of the T_m and α_m properties support their excellent reproducibility. The T_m was highly dependent on the scan rate, indicating that the thermal decomposition process was, at least in part, under kinetic control and reflects a unique thermal decomposition reaction of the drug. In contrast, the results clearly show that α_m is constant and independent of the heating rate as is well established in literature (Criado and Ortega, 1986; Sánchez-Jiménez et al., 2008). The mean α_m value obtained using the Star[®] software was 0.746 \pm 0.070 ($n=35$) whereas that calculated using Eq. (8), with different samples analysed at 1, 2.5 and 5 K/min, was 0.725 \pm 0.013 ($n=7$). These results confirm the validity of both procedures to determine α_m .

Table 3

Arrhenius parameters and 95% confidence intervals for nonisothermal decomposition of WMDF-NH₂ and its derivatives, WMD and WM, determined using the direct-differential method.

Product	Model	E_a (kJ/mol)	$\ln A$ (min^{-1})	r
WMDF-NH ₂	D1	306 [237 to 376]	74.7 [56.9 to 92.5]	0.9751
	F1	270 [220 to 321]	66.9 [54.0 to 79.9]	0.9869
	F2	276 [170 to 383]	69.3 [41.8 to 96.8]	0.9180
	F3	349 [193 to 505]	88.4 [48.2 to 129]	0.8943
	B1	62.4 [5.58 to 119]	15.7 [1.12 to 30.2]	0.7390
	P2	58.6 [0.88 to 116]	12.6 [−2.17 to 27.4]	0.7121
WMD	D1	218 [98.4 to 337]	51.1 [20.7 to 81.5]	0.8525
	F1	230 [142 to 317]	55.6 [33.4 to 77.8]	0.9495
	F2	159 [49.9 to 268]	37.9 [10.1 to 65.6]	0.7935
	F3	200 [83.6 to 315]	48.5 [19.0 to 78.1]	0.8385
	B1	−22.0 [−109 to 64.7]	−6.61 [−28.7 to 15.5]	0.2215
	P2	−7.41 [−86.6 to 101]	−1.10 [−25.0 to 22.9]	0.0702
WM	D1	377 [241 to 513]	90.0 [55.5 to 125]	0.9405
	F1	245 [213 to 276]	61.0 [53.0 to 69.1]	0.9917
	F2	271 [236 to 306]	67.9 [59.0 to 76.7]	0.9917
	F3	297 [256 to 338]	74.7 [64.2 to 85.1]	0.9905
	B1	−33.3 [−56.4 to 123]	−9.20 [−31.9 to 13.5]	0.3480
	P2	109 [93.1 to 125]	27.2 [23.1 to 31.3]	0.9892

4.3. Estimation of the activation energy (E_a), pre-exponential factor (A), and the reaction model

It is clear that in the case of a first-order reaction (F1 model), the Kissinger plot is a straight line whose slope gives the activation energy, independently of both the heating schedule used to reach the maximum reaction rate and the value of the reacted fraction α_m at this point, whereas the pre-exponential factor can be determined from the intercept. If the reaction does not follow a first-order kinetic model, the slope of the plot of $\ln(\beta/T_m^2)$ versus $1/T_m$ would only lead to the activation energy if α_m is independent of the heating schedule used. Various authors (Criado and Ortega, 1986; Budrugaic and Segal, 2007) have shown the dependence between the α_m values of the different kinetic models (Table 1) resulting from linear heating experiments and the actual value of E_a/RT . However, the error in the determination of the activation energy from the Kissinger plot has been clearly demonstrated to be lower than 5%, for values of E_a/RT higher than 10.

At first, α_m can be considered constant and independent of the linear heating rate used, and assuming first-order kinetics, the E_a obtained from Kissinger plot was 300 kJ/mol, the uncertainty being given as 95% confidence intervals calculated from the residual standard deviation by the standard expression (Draper and Smith, 1981) of 295 and 306 kJ/mol, respectively. These confidence intervals are narrow due to the large number of experimental points used. The estimated pre-exponential factor was $3.03 \times 10^{32} \text{ min}^{-1}$, the 95% confidence intervals being $6.92 \times 10^{31} \text{ min}^{-1}$ and $1.32 \times 10^{33} \text{ min}^{-1}$, respectively. These intervals are relatively small despite coupling of the uncertainty of the prediction, due to fit of the rate constants (β) at each temperature (T_m) and their dependence on the kinetic model used.

The combined analysis of experimental data by means of the logarithmic expression of the general differential equation (Eq. (4)) is thus shown to be a suitable method for determining the kinetic model and its parameters. Therefore, any set of $T-\alpha$ or $(d\alpha/dt)$ data should fit the equation, regardless of the experimental procedure used (Pérez-Maqueda et al., 2002). In order to check this, the differential method described in Section 3 was used for the kinetic analysis of data obtained from the thermal decomposition of CCK-4 at a heating rate of 5 K/min and to determine the model that best fits the data. The α (or $d\alpha/dt$) – T data were analysed by the differential method after applying the $f(\alpha)$ function proposed in the literature for describing solid-state reactions, as shown in

Table 1. Table 3 includes the resulting activation energies, the pre-exponential factors, and the correlation coefficient for the kinetic models included in Table 1. The results demonstrate that when an F1 kinetic model is assumed, all the experimental data fit by a single straight line whose slope and intercept lead to an activation energy of 270 kJ/mol and a pre-exponential factor $1.17 \times 10^{29} \text{ min}^{-1}$ with a correlation coefficient $r=0.9869$. On the other hand, for a F2 kinetic model, the apparent values of E_a and A obtained are very similar to those obtained for the F1 model, although the correlation coefficient found was lower ($r=0.9180$). The results obtained indicate that the calculated kinetic parameters were comparable to the values estimated by the Kissinger method, but the 95% confidence intervals were higher: 220–321 kJ/mol for activation energy and 2.78×10^{23} to $4.87 \times 10^{34} \text{ min}^{-1}$ for the pre-exponential factor. This discrepancy could be due to differences in the data analysis method and the lower number of degrees of freedom.

4.4. Kinetics and degradation mechanism of WMD and WM degradation products

Fig. 4 shows the reacted fraction, α , for each degradation product as a function of time. The shape of the curve is sigmoidal, as is common for solid-state decompositions; it is characterized by an induction period followed by a growth period, and finally, a decay period. In this case, the formation processes of WMD and WM have similar profiles, although the induction period for WM was slightly higher, whereas the growth period takes place at a relatively faster rate for the WMD product. This result is consistent with the observations made by Inglis (1983), since the $n-1$ cleavage is slower than $n+1$ because the former proceeds via a six-member ring intermediate rather than a five-member ring. However, the decay period was not observed for the WMD product, since the samples are totally carbonized from 220 °C, making it impossible to detect any products.

The α (or $d\alpha/dt$) – T data were analysed by means of the differential method as described earlier for CCK-4. For both products, the F1 kinetic model was found to provide the best fit to the kinetic profile. The estimated activation energies were 230 kJ/mol for WMD and 245 kJ/mol for WM, respectively. The selection of the kinetic model and calculation of the constant rates do not require knowledge of the degradation mechanism, because even complex degradation pathways involving multiple consecutive or parallel reactions can be represented by combinations of zero, first- and second-order reactions. For example, Inglis (1983) points out that $n+1$ cleavage would always precede $n-1$ cleavages; i.e. the two cleavage mechanisms occur consecutively and not in parallel. However, Joshi and Kirsch (2002) have reported for the first time that the $n-1$ cleavage can occur consecutively and in parallel to $n+1$ at Asp-residues using the polypeptide hormone glucagon as model, in acidic aqueous solution. At first, the experimental data suggest that CCK-4 degradation does not undergo a consecutive reaction, perhaps a parallel reaction; although the presence of both pathways cannot be ruled out. To investigate this, the different degradation pathways can be expressed by a system of ordinary differential equations. If the reaction is composed of two parallel steps according to the diagram in Fig. 2, then:

$$\frac{dX_1}{dt} = -(k_{12} + k_{13})X_1 = -\left(k_{T_{ref12}} \exp\left(B_{12} + \frac{E_{a12}}{R} \left(\frac{1}{T_{ref}} - \frac{1}{T(t)}\right)\right) + k_{T_{ref13}} \exp\left(B_{13} + \frac{E_{a13}}{R} \left(\frac{1}{T_{ref}} - \frac{1}{T(t)}\right)\right)\right) X_1 \quad (9)$$

$$\frac{dX_2}{dt} = k_{12}X_1 = k_{T_{ref12}} \exp\left(B_{12} + \frac{E_{a12}}{R} \left(\frac{1}{T_{ref}} - \frac{1}{T(t)}\right)\right) X_1 \quad (10)$$

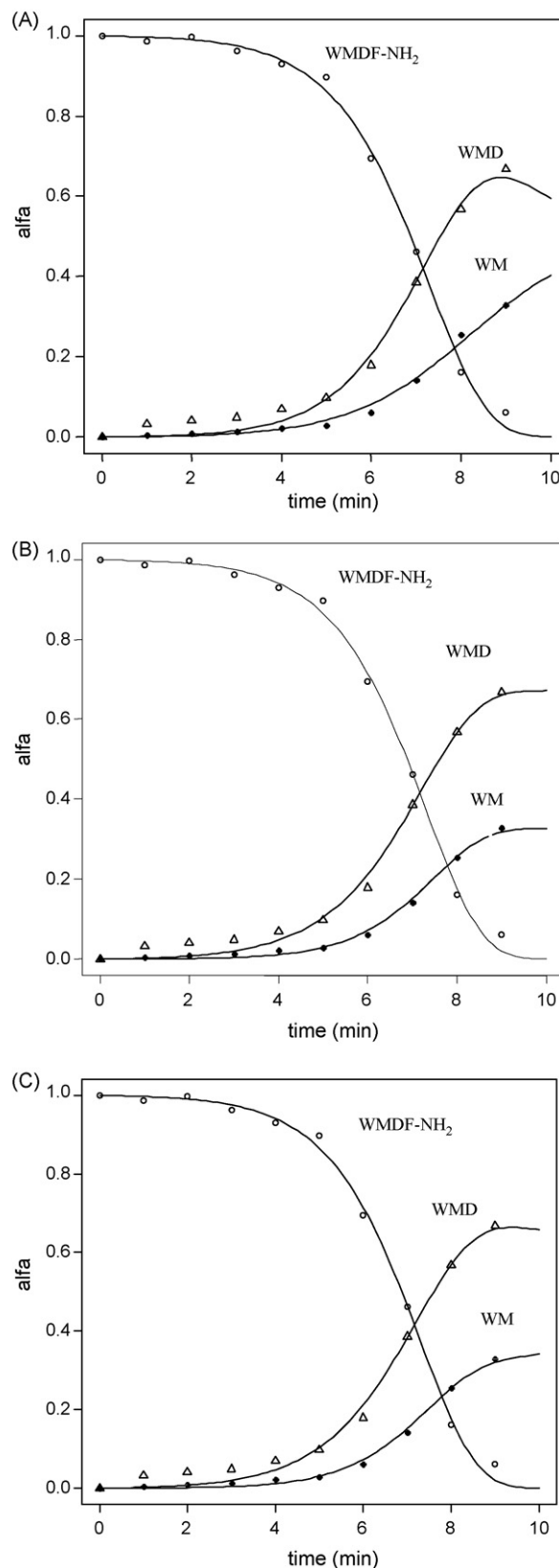


Fig. 4. Variation of the reacted fraction (α) for the products WMDF-NH₂ (open circle), WMD (triangle), and WM (black circle), respectively, vs temperature, considering a linear heating rate of 5 K/min, for the different models given in Fig. 2: consecutive reaction (A), parallel (B) and both pathways (C). Data were fitted using the R[®] statistical program through the odesolve () package.

$$\frac{dX_3}{dt} = k_{13}X_1 = k_{T_{ref13}} \exp\left(B_{13} + \frac{E_{a13}}{R} \left(\frac{1}{T_{ref}} - \frac{1}{T(t)}\right)\right) X_1 \quad (11)$$

where X_i is the amount of each product expressed as reacted fraction and k_i are rate constants with an Arrhenius-type dependence on the temperature. To reduce the strong dependence between the parameters A and E_a , the Arrhenius equation can be reformulated by introducing a reference temperature in the form:

$$k = \exp\left[B + \frac{E_a}{R} \left(\frac{1}{T_{ref}} - \frac{1}{T}\right)\right] \quad (12)$$

where the parameters of the reparameterized equations can be related to the parameters of the traditional Arrhenius equation as:

$$B = \ln(k_{T_{ref}}) \quad (13)$$

where $k_{T_{ref}}$ is the specific reaction rate at the reference temperature T_{ref} . For the rest of the schemes, the same procedure was used.

To resolve the differential equation, and estimate the kinetic parameter, the `odesolve` package from R[®] statistical program (version 2.9.0, 2009) was used, which allows a direct nonlinear estimation of the activation energy and the rate constants through `nlme()` function. This generic function fits a nonlinear mixed-effects model in the formulation described in Lindstrom and Bates (1990). The initial estimated values for E_a and the rate constants obtained by the direct-differential method were used as starting values in order to converge much faster to a solution.

Introduction of the reference temperature into the Arrhenius equation leads to reduction of the parameter correlation, consequently, less computational effort required for estimating the model parameters (Espie and Macchietto, 1988). The reference temperature is usually defined as the average of the analysed experimental data. For instance, Veglio et al. (2001) suggested that the reference temperature should be calculated as the reciprocal of the average value of the reciprocal of all the experimental temperatures. However, little attention has been given in the literature to establishing the optimum value of the reference temperature. Schwaab and Pinto (2007) showed that it is possible to determine an optimum reference temperature in order to eliminate parameter correlation and minimize the relative errors of model parameters with a single kinetic constant. The problem is more complicated when there is more than one Arrhenius equation in the model, since it then becomes necessary to define some criterion for optimization of reference temperature. Schwaab et al. (2008) used an empirical norm to resolve this problem. We propose to use the following criterion: the logarithm of the determinant of the correlation matrix of parameter estimates ($\log(\det(V))$) must be minimum. This norm is based on the asymptotic properties of correlation matrix of a multinormal random variable (Morrison, 1976).

Starting from the reference temperature of 470.2 K, calculated in accordance with Veglio et al. (2001), the application of

the norm proposed was performed, obtaining an optimum reference temperature of 479.6 K. With this reference temperature and assuming a parallel reaction, the parameter correlation, expressed as $\log(\det(V))$, was equal to -0.572 , while for $T_{ref} = 470.2$ K, the parameter correlation was equal to -4.18 . For the rest of models, the parameter correlations were always lower than the ones obtained with the average temperature of the experimental range. Although it is not possible to eliminate all the parameter correlations, the proper choice of the reference temperature can significantly reduce the final one. Similar results were obtained using the empirical norm proposed by Schwaab et al. (2008).

Fig. 4 shows the fitted curves for the different degradation pathways shown in Fig. 2. The estimated parameters and respective 95% confidence intervals obtained are presented in Table 4. The results indicate that CCK-4 degradation does not follow a consecutive reaction since the activation energy obtained for step 23 is negative and, therefore, this value lacks physical sense. However, when the data fit a parallel reaction or both consecutive and parallel process do not differ, the residual sum of squares (RSS) is slightly higher for the parallel reaction (3.714×10^{-3} vs 3.429×10^{-3}), but the increased number of parameter does not produce a significant improvement in fit. In this situation, the F -test can be used to choose between models that are hierarchical (i.e. one is the full model, and all the rest can be expressed as restricted cases of that full model), but for which there is no a priori reason to prefer one over another (Mannervik, 1981). When two models j and k with p_j and p_k ($p_j < p_k$) parameters, respectively, are fitted to the same data set and yield residual sums of squares RSS_j and RSS_k ($RSS_j > RSS_k$), the significance of the improvement in RSS by using the model (k) containing more parameters can be found by comparison of the quotient:

$$F = \left(\frac{RSS_j - RSS_k}{RSS_k}\right) \times \left(\frac{n - p_k}{p_k - p_j}\right) \quad (14)$$

with the F -statistic $F(p_k - p_j, n - p_k)$ at the appropriate significance level ($\alpha = 0.05$).

The F -test results suggest that the model with both processes offers no significant improvement over the model with the parallel reaction, since the calculated value ($F = 0.997$) is lower than the tabled value ($F = 3.40$).

Also, the confidence intervals of the estimated parameters $k_{T_{ref}}$ and E_a for step 23 corresponding to the full model include the value 0, which indicates that these parameters are not significant ($p > 0.05$) and that the consecutive reaction can be effectively disregarded. All these results indicate that the simpler model should be adopted. In this case, activation energies of 289 and 361 kJ/mol were obtained for the WMD and WM products, higher values than those obtained by the direct-differential method, but the confidence intervals of the estimated parameters are narrower. Thus, this approach gives a reliable estimate of all parameters, and this

Table 4

Estimated parameter and 95% confidence intervals using an optimized reference temperature of 479.6 K for the different degradation pathways proposed for the CCK-4 peptide shown in Fig. 2.

Parameter	Step 12	Step 13	Step 23
Both processes			
$k_{T_{ref}}$ (min^{-1})	0.246 [0.180–0.312]	0.108 [0.075–0.142]	0.0016 [–5.10 to 5.09] ^a
E_a (kJ/mol)	291 [265–318]	354 [309–400]	312 [–572 to 1196] ^a
Consecutive reaction			
$k_{T_{ref}}$ (min^{-1})	0.352 [0.345–0.359]		0.234 [0.221 to 0.249]
E_a (kJ/mol)	303 [279–327]		–81.6 [–28.7 to –134]
Parallel reaction			
$k_{T_{ref}}$ (min^{-1})	0.244 [0.237–0.251]	0.110 [0.100–0.120]	
E_a (kJ/mol)	289 [262–316]	361 [299–424]	

^a Probability > 0.05.

fact is reflected in the goodness of fit between experimental data and the kinetic model adopted.

To evaluate the effect of heating rate on degradation mechanism of CCK-4 peptide, a second experiment was conducted under a linear heating rate of 2.5 K/min. The results obtained seem to confirm that the in-parallel reaction is the most probable, and therefore, the degradation pathway is independent of the heating rate.

5. Conclusions

The DSC analysis of CCK-4 peptide showed two endothermic peaks, attributed to the decomposition and the melting, respectively. Degradation products, WMD and WM, were identified by proteolytic digestion and MALDI-TOF mass spectrometry. This result suggests that the degradation pathway involves the cleavage reaction on the $n - 1$ and $n + 1$ sides of aspartic acid.

The nonisothermal kinetic analysis was carried out using the Kissinger method, which requires two conditions: a first-order kinetic model and that the reacted fraction at the maxima remains unchanged. At first, both requirements are fulfilled, obtaining activation energy of 300 kJ/mol. However, this method provides little data on reaction complexity.

The direct-differential method can offer an alternative approach for determining kinetic parameters and the reaction model since it can be used to analyse experimental data obtained under the same or different conditions. For this, the kinetics of CCK-4 degradation were also studied from a data set generated under linear heating at a constant rate of 5 K/min. The activation energy and pre-exponential factor determined by the differential method were found to be in good agreement with the results of Kissinger's method. In any case, the activation energy for the solid-state reaction is much greater than that in solution (102 kJ/mol) (Oliva et al., 2006a), reflecting the greater energy required for rearrangement within the confines of a crystal lattice.

The cleavage reaction at the Asp-residue occurs on both N- and C-terminal sides, but the mechanism can occur through consecutive or parallel reactions, or both. To investigate this, a system of differential equations appropriate for each scheme was analysed using the R[®] statistical program. In this case, the reparameterization of the Arrhenius equation and the proper choice of a reference temperature are crucial to improve the precision of the estimated parameters. A slightly better fit was obtained for a scheme involving both processes, since the RRS was lower; however, the *F*-test results suggest that this scheme offers no significant improvement over the parallel reactions. In view of the results, pharmaceutical researchers are challenged to gain a better understanding of the models, statistical and mathematical tools and software that can be applied in studying solid-state reaction kinetics.

In summary, these results indicate that the nonisothermal methodology used in this study may be used to extrapolate peptide and protein stability in the solid-state, saving time, samples and experimental effort. Also, proteins in the dry state, even if formulated with disaccharides, are thermodynamically unstable at normal storage temperatures (Pikal et al., 2008), so they would be a representative example to evaluate the practical potential of the methodology applied in this study. This is a future research topic in our laboratory.

6. Nomenclature

A	pre-exponential factor (min^{-1})
E_a	activation energy (kJ/mol)
$f(\alpha)$	reaction model

n	reaction order
R	gas constant (J/mol K)
T	absolute temperature (K)
t	time (min)
m	sample weight
k	rate constant (min^{-1})
T_m	temperature at maximum rate (K)
T_{ref}	optimum reference temperature (K)
X_i	amount of each product expressed as reacted fraction
RSS	residual sum of squares

Greek letters

α	reacted fraction
α_m	reacted fraction at maximum temperature
β	linear heating rate (K/min)

Acknowledgments

The authors would like to thank Laura Colombo (Istituto di Ricerche Farmacologiche "Mario Negri", Milan, Italy) for providing the WMD and WM peptides for this study. This research has been financed by the Fondo de Investigación de la Seguridad Social, Spain as part of project PI 061804.

References

- Abd-Elrahman, M.I., Ahmed, M.O., Ahmed, S.M., Aboul-Fadl, T., El-Shorbagi, A., 2002. Kinetics of solid state stability of glycine derivatives as a model for peptides using differential scanning calorimetry. *Biophys. Chem.* 97, 113–120.
- Anonymous, 2005. International Conference on Harmonization (ICH) of Technical Requirements for the Registration of Pharmaceuticals for Human Use, Validation of Analytical Procedures: Text and Methodology (ICH-Q2-R1), November 2005.
- Beezer, A.E., Gaiford, S., Hills, A.K., Wilson, R.J., Mitchell, J.C., 1999. Pharmaceutical microcalorimetry: application to long-term stability studies. *Int. J. Pharm.* 179, 159–165.
- Budrugeac, P., Segal, E., 2007. Applicability of the Kissinger equation in thermal analysis revisited. *J. Therm. Anal. Calorim.* 88, 703–707.
- Burnham, K., 2000. Computational aspects of kinetic analysis. Part D: the ICTAC kinetics project—multi-thermal-history model-fitting methods and their relation to isoconversional methods. *Thermochim. Acta* 355, 165–170.
- Capelle, M.A.H., Gurny, R., Arvinte, T., 2007. High throughput screening of protein formulation stability: practical considerations. *Eur. J. Pharm. Biopharm.* 65, 131–148.
- Criado, J.M., Ortega, A., 1986. Analysis of the shape index of DTG or DTA curves under hyperbolic or logarithmic schedule. *Thermochim. Acta* 103, 317–323.
- Draper, N., Smith, H., 1981. *Applied Regression Analysis*, second edition. Wiley, New York.
- Elder, J.P., 1985. The general applicability of the Kissinger equation in thermal analysis. *J. Therm. Anal.* 30, 657–669.
- Espie, D.M., Macchietto, S., 1988. Nonlinear transformations for parameter estimation. *Ind. Eng. Chem. Res.* 27, 2175–2179.
- Ford, J.L., Timmins, P., 1989. *Pharmaceutical Thermal Analysis, Techniques and Application*. Ellis Horwood, Chichester.
- Giron, D.J., 2002. Applications of thermal analysis and coupled techniques in pharmaceutical industry. *J. Therm. Anal. Calorim.* 68, 335–357.
- Gotthard, M., Boermann, O.C., Behr, T.M., Behe, M.P., Oyen, W.J., 2004. Development and clinical application of peptide-based radiopharmaceuticals. *Curr. Pharm. Des.* 10, 2951–2963.
- Inglis, A.S., 1983. Cleavage at aspartic acid. *Methods Enzymol.* 91, 324–332.
- Joshi, A.B., Kirsch, L.E., 2002. The relative rates of glutamine and asparagine deamidation in glucagons fragment 22–29 under acidic conditions. *J. Pharm. Sci.* 91, 2332–2345.
- Khawam, A., Flanagan, D.R., 2006a. Basics and applications of solid-state kinetics: a pharmaceutical perspective. *J. Pharm. Sci.* 95, 472–498.
- Khawam, A., Flanagan, D.R., 2006b. Solid-state kinetic models: basics and mathematical fundamentals. *J. Phys. Chem. B* 110, 17315–17328.
- Lai, M.C., Topp, E.M., 1999. Solid-state chemical stability of proteins and peptides. *J. Pharm. Sci.* 88, 489–500.
- Lindstrom, M.J., Bates, D.M., 1990. Nonlinear mixed effects models for repeated measures data. *Biometrics* 46, 673–687.
- Mannervik, B., 1981. Design and analysis of kinetic experiments for discrimination between rival models. In: Endrenyi, L. (Ed.), *Kinetic Data Analysis: Design and Analysis of Enzyme and Pharmacokinetic Experiments*. Plenum Press, New York, pp. 235–270.
- Morrison, D.F., 1976. In: Arthur, A., Gardner, M. (Eds.), *Multivariate Statistical Methods*, second edition. McGraw Hill, New York.

- Mu-Lan, L., Stavchansky, S., 1998. Isothermal and nonisothermal decomposition of thymopentin and its analogs in aqueous solution. *Pharm. Res.* 15, 1702–1707.
- Oliva, A., Llabrés, M., Fariña, J.B., 2006a. Data analysis of kinetic modelling used in drug stability studies: isothermal versus nonisothermal assays. *Pharm. Res.* 23, 2595–2602.
- Oliva, A., Hidalgo, M., Alvarez, C., Llabrés, M., Fariña, J.B., 2006b. Evaluation of cholecystokinin (CCK-8) peptide thermal stability for use as radiopharmaceutical by means isothermal and nonisothermal approaches. *Drug Dev. Ind. Pharm.* 32, 947–953.
- Ozawa, T., 2000. Kinetic analysis by repeated temperature scanning. Part 1. Theory and methods. *Thermochim. Acta* 356, 173–180.
- Pérez-Maqueda, L.A., Criado, J.M., Otor, F.J., Málek, J., 2002. Advantages of combined kinetic analysis of experimental data obtained under any heating profile. *J. Phys. Chem. A* 106, 2862–2868.
- Pikal, M.J., Rigsbee, D., Roy, M.L., 2008. Solid state stability of proteins III: calorimetric (DSC) and spectroscopic (FTIR) characterization of thermal denaturation in freeze dried human growth hormone (hGH). *J. Pharm. Sci.* 97, 5122–5131.
- Roduit, B., 2000. Computational aspects of kinetic analysis. Part E: the ICTAC kinetics project-numerical techniques and kinetics of solid state processes. *Thermochim. Acta* 355, 171–180.
- Sánchez-Jiménez, P.E., Criado, J.M., Pérez-Maqueda, L.A., 2008. Kissinger kinetic analysis of data obtained under different heating schedules. *J. Therm. Anal. Calorim.* 94, 427–432.
- Schwaab, M., Pinto, J.C., 2007. Optimum reference temperature for reparameterization of the Arrhenius equation. Part 1: problems involving one kinetic constant. *Chem. Eng. Sci.* 62, 2750–2764.
- Schwaab, M., Lemos, L.P., Pinto, J.C., 2008. Optimum reference temperature for reparameterization of the Arrhenius equation. Part 2: problems involving multiple reparameterizations. *Chem. Eng. Sci.* 63, 2895–2906.
- Statistics Department of the University of Auckland, 2009. *Statistical Data Analysis R*, version 2.9.0. Auckland, USA., www.r-project.org.
- Veglio, F., Trifoni, M., Pagnanelli, F., Toro, L., 2001. Shrinking core model with variable activation energy: a kinetic model of manganiferous ore leaching with sulphuric acid and lactose. *Hydrometallurgy* 60, 167–179.
- Vyazovkin, S., 2004. Thermal analysis. *Anal. Chem.* 7, 3299–3312.
- Vyazovkin, S., Wight, C.A., 1999. Model-free and model-fitting approaches to kinetic analysis of isothermal and nonisothermal data. *Thermochim. Acta* 340, 53–68.